Sakarya Üniversitesi Fen Bilimleri Dergisi
Sakarya University Journal of Science

e-ISSN : 2147-835X
Publisher : Sakarya University

Vol. 30, No. 3, 383-395, 2026
DOI: https://doi.org/10.16984/saufenbilder.1839948

Research Article

Eco-Friendly Chitosan-Based Composite for Superior Pb^{2+} Adsorption: Mechanism and Performance İnsights

Bayram Aygün[1], Zeynep Mine Şenol[1*]

[1]Sivas Cumhuriyet University, Faculty of Science, Department of Nutrition and Diet, Sivas, Türkiye, bayramaygn60@gmail.com, msenol@cumhuriyet.edu.tr

*Corresponding Author

ARTICLE INFO

Keywords:
Chitosan
Alginate
Composite beads
Pb^{2+} removal
Wastewater treatment

Article History:
Received: 10.12.2025
Revised: 27.01.2026
Accepted: 21.04.2026
Online Available: 29.06.2026

ABSTRACT

The presence of Pb^{2+} ions in water systems poses severe environmental and public health hazards, highlighting the need for efficient and sustainable treatment technologies. Among various remediation approaches, adsorption stands out due to its practicality and cost-effectiveness; however, selecting environmentally benign, highly efficient, and low-cost adsorbents remains a key challenge. In this work, composite beads of the biopolymers chitosan (Ch) and alginate (A) were synthesized to address this need. After synthesis, the structural characteristics of the Ch–A beads were examined, and their adsorption performance toward Pb^{2+} ions was systematically evaluated under varying operational parameters. The results indicated that the composite beads removed Pb^{2+} ions efficiently while maintaining structural stability. The adsorption mechanism was governed mainly by chemical interactions, and the composite achieved a maximum adsorption capacity of 279 mg g^{-1}. Thermodynamic and kinetic analyses confirmed that adsorption occurred via endothermic and spontaneous processes and was controlled by multiple pathways, including pore and film diffusion. Overall, these findings demonstrate that Ch–A composite beads provide a scalable, environmentally sustainable, and regenerable adsorbent material suited for removing Pb^{2+} ions from contaminated water.

1. Introduction

In recent years, the rapid expansion of industrial activities, particularly in sectors such as leather processing, mining, battery production, and electroplating, has led to a significant increase in the discharge of wastewater contaminated with Pb^{2+} ions into the environment [1, 2]. Lead, a non-biodegradable and highly toxic heavy metal, is generally present in aquatic systems in its divalent ionic form, which readily binds to biomolecules and activates various enzymatic and metabolic pathways [3]. Lead is not biodegradable and tends to accumulate in living organisms, making it a serious environmental and public health problem [4].

The tendency of Pb^{2+} ions to accumulate in living organisms makes it a particularly hazardous pollutant with toxic, mutagenic, and carcinogenic effects on human health [5]. Because of these serious health and environmental risks, the World Health Organization (WHO) has set the maximum acceptable concentration of Pb^{2+} in drinking water at 10 µg L^{-1} [6]. Considering its toxicity and persistence, Pb^{2+} removal from industrial wastewater is of vital importance for environmental protection and human health. Various physicochemical treatment methods, including ion exchange, chemical precipitation, reverse osmosis, membrane filtration, adsorption, and electrochemical processes, have been used to remove Pb^{2+} ions from wastewater [7, 8].

However, despite their effectiveness, most of these methods suffer from problems such as high operating costs, energy requirements, secondary

Cite as: Z.M. Şenol, "Eco-Friendly chitosan-based composite for superior Pb^{2+} adsorption: mechanism and performance insights," *Sakarya University Journal of Science*, vol. 30, no. 3, pp. 383-395, 2026. https://doi.org/10.16984/saufenbilder.1839848

This is an open access paper distributed under the terms and conditions of the Creative Commons Attribution-NonCommercial 4.0 International License.

pollution, or technical complexity. Adsorption, as a sustainable alternative, has emerged as a promising method for heavy metal removal due to its advantages, including simplicity, cost-effectiveness, low energy requirements, high efficiency, environmental friendliness, and the potential for adsorbent regeneration and reuse [9]. In adsorption methods, the selection of appropriate adsorbents is crucial [10]. The physicochemical and morphological properties of the adsorbents used largely influence the performance of adsorption processes. Biopolymer-based materials and composites are attracting increasing interest due to their environmental compatibility, functional versatility, and tunable surface properties. In this context, polysaccharides such as chitosan and alginate, which are natural biopolymers, have emerged as promising candidates for the development of efficient adsorbents.

Chitosan, a low-cost, non-toxic, biodegradable, sustainable, and hydrophilic biopolymer, offers active binding sites with high affinity for heavy metal ions thanks to the hydroxyl (-OH) and amino ($-NH_2$) groups in its polymer chain [11]. However, chitosan has some disadvantages, such as low mechanical strength, limited specific surface area, high swelling behavior, susceptibility to agglomeration, and proneness to degradation in acidic environments [12]. On the other hand, sodium alginate is a natural polysaccharide extracted from brown algae. It possesses some superior properties, such as high biocompatibility, biodegradability, and renewability. It also contains -OH and -COOH groups, which have high adsorption affinity for heavy metal ions [13]. However, sodium alginate's mechanical strength, stability, and heat resistance are disadvantages [14]. The use of chitosan and alginate as a composite material offers a renewable, environmentally friendly alternative for green chemistry and efficient heavy metal removal.

In this study, cross-linked Ch-A composite beads were successfully synthesized using epichlorohydrin (ECH) and sodium tripolyphosphate (NaTPP) using an innovative approach for the effective removal of Pb^{2+} ions from aqueous media. The novelty of this study is that the composite structure, developed by combining two different cross-linkers, exhibited superior mechanical stability and surface functionality. The Pb^{2+} removal performance was investigated in detail depending on the adsorption conditions, and the adsorption mechanisms were explained in depth through kinetic, isotherm, and thermodynamic analyses. By analyzing structural and surface properties using comprehensive characterization techniques such as FT-IR, SEM-EDX, and the point of zero charge (pH_{pzc}), the relationship between material properties and Pb^{2+} heavy metal removal capacity has been clearly demonstrated. In this context, the study offers significant contributions to the literature on Pb^{2+} removal through its unique synthetic approach, the synergistic effect of double cross-linker hybrid structures, and comprehensive analyses.

2. General Methods

2.1. Chemicals

In this study, sodium alginate and chitosan (medium molecular weight) were supplied by Merck (Germany), and ECH, NaTPP, HCl, C_2H_5OH, NaOH, and other chemicals were supplied by Sigma–Aldrich (produced in Iceland).

2.2. Synthesis of Ch-A adsorbent

2 g of chitosan and 2 g of alginate were added to 50 mL of 5% acetic acid. The mixture was then stirred on a magnetic stirrer for 2 hours to ensure homogeneity. 80 mL of ECH, a crosslinker, was then added and stirred for 1 hour. Then, the Ch-A mixture crosslinked with ECH was added to the NaTPP solution. The composite beads were soaked in this solution overnight. Then, the formed Ch-A composite beads were washed with plenty of pure water until neutrality was achieved, then filtered and left to dry at room conditions. Crosslinked Ch-A composite beads were prepared in this way (**Figure 1**). The characterization of this new adsorbent was performed; the performance of the prepared adsorbent in removing Pb^{2+} ions was evaluated using different experimental conditions.

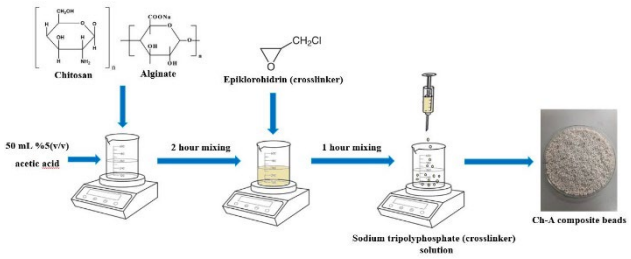


Figure 1. Schematic representation of the synthesis of Ch-A composite beads

2.3. Experimental Design and Parameter Effects

The adsorption performance of the Ch-A composite in the removal of Pb^{2+} ions was investigated using a batch biosorption experimental method with different parameters such as medium pH (2.0-5.0), initial Pb^{2+} ion concentration (50-1000 mg L^{-1}), time (0-1440 min), temperature (5 °C, 25 °C and 40 °C) and Ch-A adsorbent amount (1-20 g L^{-1}). Adsorption studies were carried out in 10 mL polypropylene tubes containing 50 mg Ch-A and a constant Pb^{2+} concentration of 1000 mg L^{-1} in 10 mL of solution. Samples were incubated at 25 °C for 24 hours. After the adsorption process, the supernatant was filtered, and the absorbances of the metal complexes formed with PAR at a wavelength of λ = 518 nm were determined using a UV-vis spectrophotometer [5]. The percentage of Pb^{2+} removal (Removal% %), and the adsorption capacity (Q, mg g^{-1}) were calculated using Eq. 1 and Eq. 2, respectively.

$$Removal\% = \left[\frac{C_i - C_f}{C_i}\right] 100 \qquad (1)$$

$$Q = \left[\frac{C_i - C_f}{m}\right] V \qquad (2)$$

Here, C_i (mg L^{-1}) and C_f (mg L^{-1}) represent the initial and equilibrium dye concentrations, respectively, while m (mg) is the mass of the adsorbent and V (L) is the volume of the solution.

3. Results and Discussion

3.1. FT-IR and SEM-EDX Analysis

To confirm that the Ch-A composite was successfully synthesized (**Figure 2**). The FT-IR spectra of Ch, A, Ch-A, and the Pb^{2+} adsorbed Ch-A composite are presented comparatively in Figure 1. When the FT-IR spectrum of alginate ($C_6H_{10}O_7$) is examined, peaks indicating the presence of carboxylate groups and hydroxyl groups, which characterize its chemical structure, are observed. Typically, a broad -OH stretching band in the 3100-3600 cm^{-1} range is observed in the alginate spectrum, while the peaks at 2918 and 1593 cm^{-1} are attributed to aliphatic C-H stretching. The peaks at 1593 and 1415 cm^{-1} are attributed to asymmetric and symmetric $-COO^-$ stretching vibrations. The peaks at 1093 and 1040 cm^{-1} are attributed to -C-O-C- stretching vibrations of ether and alcohol groups [15, 16].

In the FT-IR spectrum of chitosan, an OH stretching band is observed in the range of 3400-3500 cm^{-1}, an amide I band (C=O stretching) around 1650 cm^{-1}, and an amide II band (N-H bending) around 1550 cm^{-1}. In addition, C-O-C stretching vibrations are observed in the range of 1150-1070 cm^{-1} [17]. In the Ch-A composite, it is seen that both of its components show characteristic peaks, which is evidence that the Ch-A composite has been successfully synthesized. The co-occurrence of characteristic peaks of chitosan and alginate in the Ch-A composite spectrum confirms structural integration.

The observed shifts and intensity changes in the -COO- band around 1600 cm^{-1} and the -NH band around 1550 cm^{-1} indicate electrostatic interaction between the $-NH_3^+$ groups of chitosan and the $-COO^-$ groups of alginate. The increase/shift in the C-O-C bands and decrease in the broad -OH band in the 1100-1150 cm^{-1} region as a result of cross-linking with ECH suggest the formation of covalent ether bridges via hydroxyl groups. Furthermore, band contributions due to P=O and P-O vibrations in the 1150-1250 cm^{-1} range and changes in the 1500-1650 cm^{-1} region reveal the ionic interaction of TPP with the $-NH_3^+$ groups. These findings demonstrate the simultaneous presence of both covalent (ECH-derived) and ionic (TPP-COO^-/-NH_3^+ interactions) cross-linking mechanisms in the composite.

When the FT-IR spectrum after Pb^{2+} ion adsorption is compared with that of the Ch-A composite, the increases in peak intensities are remarkable while the peak locations remain unchanged, which is evidence of Pb^{2+} adsorption.

The observed shifts in the $–COO^-$ (1600–1400 cm^{-1}), -NH, and C-O-C bands after Pb^{2+} adsorption indicate that metal ions coordinate with carboxylate, amino, and hydroxyl groups. Furthermore, the presence of phosphate groups suggests that a multiple binding mechanism (ion exchange and surface complexation) occurs, contributing to complexation with Pb^{2+} ions. This structurally supports the high metal-binding capacity of the composite.

SEM morphologies and EDX spectra of the composites Ch, A, and Ch-A are presented in **Figure 3**, and Pb^{2+} adsorbed Ch-A is presented in **Figure 4** for comparison. From the SEM morphologies, it is seen that Ch has a porous and smooth surface, while alginate has a homogeneous surface and a more irregular shape with cracks [18]. The SEM image of the Ch-A composite has a completely different morphology from its components. The porous surface morphology of chitosan created fluctuations with the incorporation of alginate into the structure. These morphological changes indicated that chitosan interacted well with alginate, and the surface morphologies were modified by physicochemical interactions. The formation of Ch-A composite beads increased the interaction between the carbonyl groups of alginate and the amine groups of chitosan. The new texture in the SEM image of the Ch-A composite is a result of electrostatic interactions. It is also noticeable that the surface morphology of the Ch-A composite changed significantly after Pb^{2+} adsorption.

The Ch-A composite surface appears to have become smoother after Pb^{2+} ion adsorption, indicating surface complexation. EDX spectra **(Figure 3)** showed that Ch contained C, N, and O, while alginate contained C, O, and Na. The Ch-A composite contained C, N, O, and Na, elements found in both Ch and alginate. Furthermore, EDX analyses of the Ch-A composite indicated that chitosan had been incorporated into the alginate structure, as evidenced by the presence of N in the composite beads.

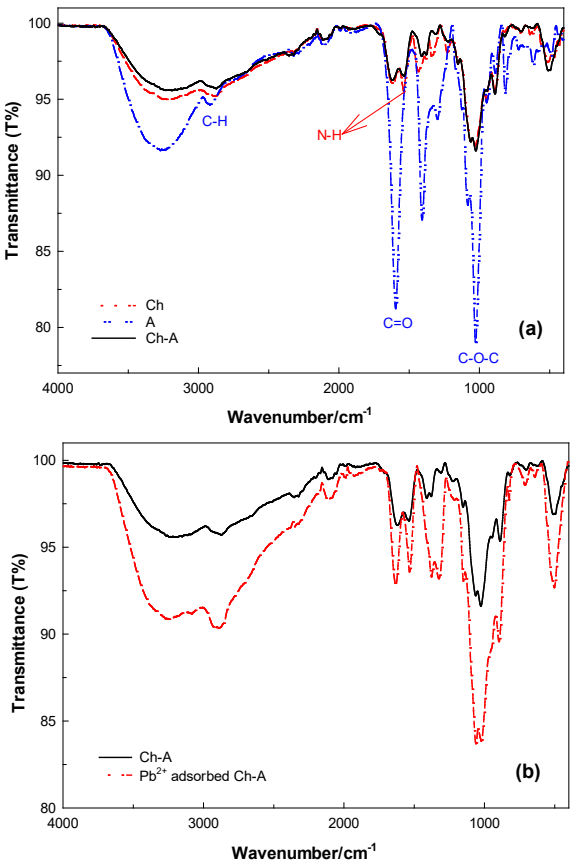


Figure 2. FT-IR spectra for Ch, A, Ch-A, (a) and Pb^{2+} adsorbed Ch-A composite (b)

The presence of Pb in the EDX spectrum of the Ch-A composite adsorbed with Pb^{2+} ions (**Figure 4**), in addition to the elements present in the composite structure (C, N, and O), is considered evidence of metal adsorption. Furthermore, the disappearance of the Na peaks in the EDX spectrum of the Ch-A composite after Pb^{2+} adsorption provides strong evidence of an ion-exchange mechanism. The replacement of the Na^+ ions initially present in the composite matrix with Pb^{2+} ions supports the significant contribution of ion exchange to the overall adsorption process.

3.2. Effect of Initial pH and the pH_{pzc} for Ch-A

The pH of the aqueous solution plays a critical role in the adsorption processes by affecting both the ionization state of the adsorbent surface and the chemical form of the adsorbate species. **Figure 5** shows the change in Pb^{2+} ion removal concerning pH. The effect of pH on the adsorption process was investigated by varying the pH in the range of 1.0-5.0 while keeping other parameters ($[Pb^{2+}]_0$: 1000 mg L^{-1}, m: 5 g L^{-1}, t:

24 h, T: 25 °C) constant, and the results are presented in **Figure 5**.

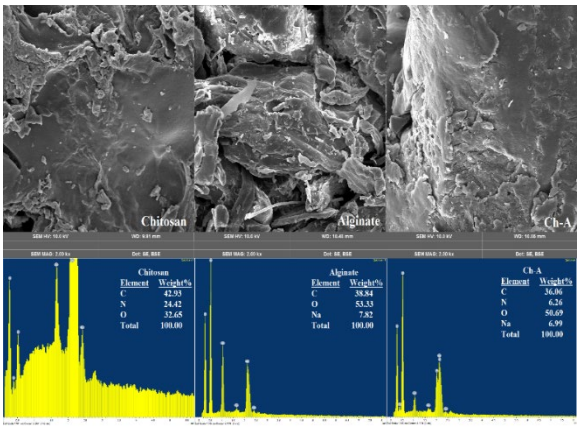


Figure 3. SEM morphologies of Ch, A, Ch-A composite, and EDX spectra

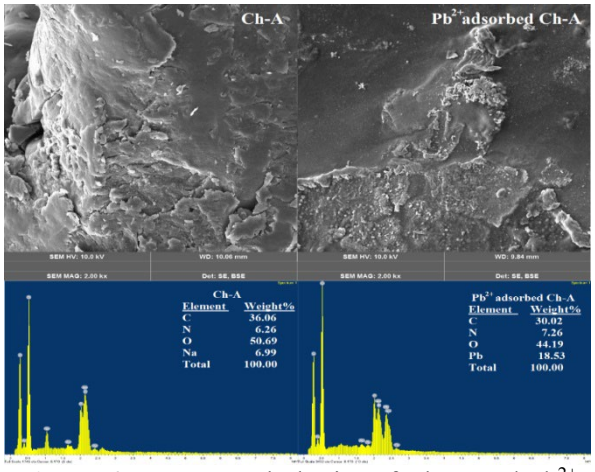


Figure 4. SEM morphologies of Ch-A and Pb^{2+} adsorbed Ch-A composite, and EDX spectra

As seen in Figure 3, the adsorption efficiency of the Ch-A composite increased with increasing solution pH. Pb^{2+} ion adsorption is affected by the ambient pH. At acidic pH values, protonation of amine and carboxyl groups causes a decrease in Pb^{2+} ion adsorption. At acidic pH values, the presence of more H^+ ions than Pb^{2+} ions causes protonation at the active centers on the Ch-A surface to become positively charged, thus decreasing the adsorption efficiency of Pb^{2+} ions. Competitive bonding between Pb^{2+} and H^+ ions decreases with increasing pH. Pb^{2+} ion adsorption increases with increasing pH.

As pH increases, the number of H^+ ions decreases, allowing Pb^{2+} ions to interact more easily with functional groups such as amines, carboxyls, and hydroxyls on the Ch-A composite; these groups begin to deprotonate and become negatively charged. In this case, electrostatic interactions with Pb^{2+} ions on the adsorbent surface increase, which also increases adsorption efficiency. Furthermore, at pH 4.5, where complexation is also effective, it also plays a role in increasing adsorption capacity. Pb^{2+} ion adsorption was found to be 25% at pH 1, 65% at pH 2, 71% at pH 3, 89% at pH 4, and 85% at pH 5. Many articles have reported similar effects of pH on Pb^{2+} adsorption [19]. At pH>6.0, Pb^{2+} ions produce $Pb(OH)^+$ and $Pb(OH)_2$ precipitates [20]. At these pH values, precipitation was not studied because it could be perceived as adsorption. The natural pH of Pb^{2+} ions was used in all adsorption experiments.

The point of zero charge value of the adsorbent is a critical parameter for understanding and interpreting electrostatic interactions during adsorption processes. Knowing the charge of the adsorbent in a given pH range plays a vital role in predicting the binding behavior of target contaminants (e.g., metal ions, dyes, etc.) to the surface. The pHpzc value of the Ch-A composite was determined using the solid addition method [21], and the pHpzc of the composite was determined to be 4.6 (**Figure 5**). At solution pHs lower or higher than this pH value, the surface charge of the composite changes, and this directly affects the adsorption process of Pb^{2+} ions.

When pHsolution<pHpzc, the Ch-A surface is positive, and since the Pb^{2+} ions present in the medium are also positively charged, electrostatic repulsion occurs between them. This makes it difficult for Pb^{2+} ions to adhere to the Ch-A surface. When pHsolution>pHpzc, the Ch-A surface is negative, and the Pb^{2+} ions present in the medium are attracted to the composite surface by electrostatic attraction. This facilitates the adhesion of Pb^{2+} ions to the Ch-A surface. The pH_{pzc} value of Ch-A composite is consistent with the experimental findings explaining the pH effect on the adsorption process.

3.3. Effect of Adsorbent Dose

Figure 6 shows the change in Pb^{2+} ion removal depending on the adsorbent dose. The adsorbent dose was varied within the range of 1-20 g L^{-1}, while other parameters ($[Pb^{2+}]_0$: 1000 mg L^{-1}, pH: 4.5, t: 24 h, T: 25 °C) were kept constant. As

seen in **Figure 6**, the Pb^{2+} removal percentage increased from 55% to 86% as the adsorbent dose increased. This is due to the increase in the active centers on the composite surface with the increasing adsorbent amount. The presence of more adsorptive sites on the adsorbent surface increases the Pb^{2+} removal efficiency.

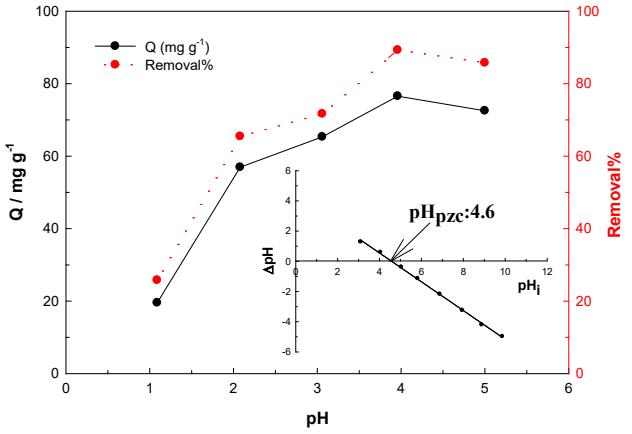


Figure 5. Effect of pH

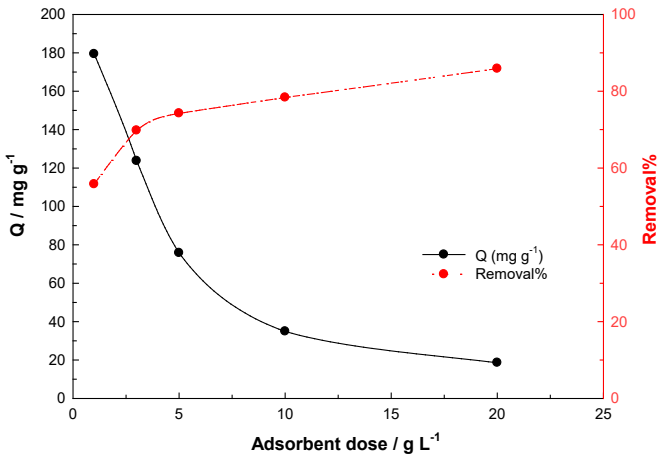


Figure 6. Effect of adsorbent dose

3.4. Modeling of Adsorption Process

The effect of concentration on the adsorption of Pb^{2+} ions onto Ch-A composite was investigated in the concentration range of 50-1000 mg L^{-1} by keeping other parameters (m: 5 g L^{-1}, pH: 4.5, t: 24 h, T: 25 °C) constant. To optimize the design of the Pb^{2+} ions adsorption process onto the adsorbent, three different isotherm models were used to explain the relationship between Pb^{2+} concentrations in the solid-liquid phase. In this study, the experimental data were based on the methods of Langmuir [22], Freundlich [23], and Dubinin-Radushkevich (D-R) [24] were applied to the non-linear equations of the isotherm models (**Table 1**).

Figure 7 shows the fit of the isotherm models for Pb^{2+} ion removal. As **Figure 7** shows, as the Pb^{2+} ions concentration increases, the Pb^{2+} adsorption capacity of the Ch-A composite increases rapidly, from 4.60 mg g^{-1} to 69.8 mg g^{-1}. This is because, when the solution concentration is low, the active centers in the Ch-A composite are not fully occupied, resulting in a lower adsorption capacity. However, as the Pb^{2+} concentration in the solution increases, the active centers on the composite surface are gradually occupied by Pb^{2+} ions, increasing the adsorption capacity. When the active centers are completely occupied, the adsorption capacity reaches equilibrium.

The R^2 values in **Table 1** showed that the Langmuir model was more consistent with the concentration data. This indicated that the adsorption of Pb^{2+} ions onto the Ch-A composite was a monolayer process. The maximum adsorption capacity from this model was found to be 279 mg g^{-1}. The Ch-A composite adsorbent has homogeneous Pb^{2+} ions on its surface, and the adsorption behavior follows a single-layer adsorption mechanism on a homogeneous surface. Using the Langmuir model, the adsorption capacity was determined to be 279 mg g^{-1}.

The Freudlich model, which describes the multilayer adsorption process on a heterogeneous surface, yielded a value of X_F, a measure of adsorption capacity, of 0.206, and a surface heterogeneity of β of 0.852. The D-R isotherm allows the calculation of the adsorption energy (E_{DR}), which provides information about the physical and chemical characteristics of adsorption. If the adsorption energy E_{DR}<8 kJ mol^{-1}, the adsorption process is dominated by physical adsorption; if E_{DR}= 8–16 kJ mol^{-1}, ion exchange and complex formation; and if E_{DR}>16 kJ mol^{-1}, particle diffusion [25]. E_{DR}=9.51 kJ mol^{-1} was found, indicating that the adsorption process is chemical, and ion exchange and complex formation dominate the adsorption.

When the comparative data presented in **Table 2** are examined, it is seen that the Pb^{2+} removal capacity of Ch-A composite beads (279 mg g^{-1}) is quite high compared to many adsorbents reported in the literature. These results clearly demonstrate that the synthesized Ch-A

composite beads are a competitive and superior alternative to many adsorbents in the literature in terms of Pb^{2+} removal.

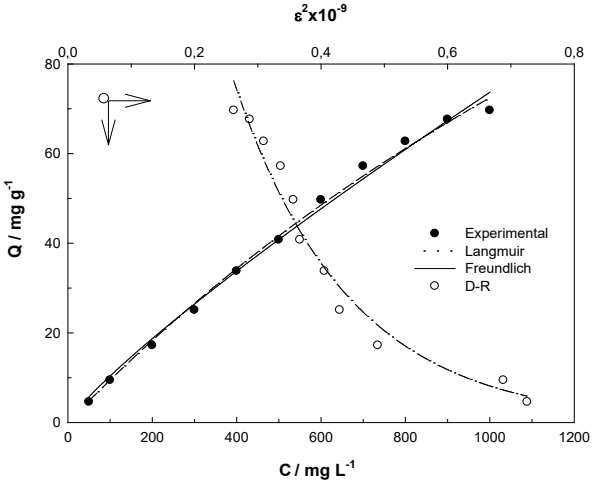


Figure 7. Adsorption isotherm models

Table 1. Parameters of isotherm models

Isotherm Model	Parameter	Value
Langmuir	Q_L (mg g^{-1})	279
$Q = \frac{Q_L C_e}{1 + K_L C_e}$	$K_{Lx}10^3$ (L mg^{-1})	0.352
	R^2	0.996
Freundlich	X_F	0.206
$Q = X_F C_e^{\beta}$	β	0.852
	R^2	0.993
D-R	X_{DR} (mg g^{-1})	325
$Q = X_{DR} e^{-(K_{DR}\varepsilon^2)}$	$-K_{DR}x10^9$/mol^2 KJ^{-2}	5.53
$\varepsilon = RT\ln\left(1 + \frac{1}{C_e}\right)$	E_{DR}/kJ mol^{-1}	9.51
$E_{DR} = (2K_{DR})^{-0.5}$	R^2	0.967

3.5. Effect of Contact Time on Adsorption

The effect of contact time on Pb^{2+} adsorption onto Ch-A composite was investigated in the time range of 10-1440 min by keeping other parameters ($[Pb^{2+}]_0$: 1000 mg L^{-1}, m: 5 g L^{-1}, pH: 4.5, T: 25 °C) constant. **Figure 8** shows the change in Pb^{2+} ion removal with time. When **Figure 8** is examined, it is seen that the effect of contact time on Pb^{2+} ion adsorption onto Ch-A composite occurs in three stages. i) The first stage is rapid (10-60 min) and is attributed to external surface Pb^{2+} adsorption. Pb^{2+} removal increased rapidly within the first 60 min.

This is due to the presence of a large number of active centers on the composite surface and the rapid filling of these sites. ii) The second stage (60-480 min) is attributed to intraparticle diffusion resulting from the adsorption of Pb^{2+} ions within the pores of the Ch-A. At this stage, removal efficiency gradually decreases. iii) The third stage (480-1440 min) is the stage where adsorption equilibrium occurs.

Table 2. Pb^{2+} ion uptake capacities of various adsorbent materials

Adsorbent	pH	Q / mg g^{-1}	Ref.
Chitosan-derived copolymeric blend	6.0	177	[26]
Jackfruit peel-derived biochar	5.7	83.86	[27]
Fe_3O_4-CS/EDTA	6.0	220.0	[28]
Polymer-grafted silica-coated acid-resistant magnetic chitosan	6.0	88.03	[29]
Chitosan/fluorapatite biocomposite	4.0	60.24	[30]
Chitosan-conjugated magnetite nanoparticle	6.1	192.3	[31]
Calcined modified attapulgite	-	84.64	[32]
Graphene oxide@sodium alginate	-	241.5	[33]
Porous geopolymers	6.0	85.67	[34]
Polyphenol-analogous dextran hydrogel	-	102.35	[35]
Cs Schiff base@Fe/NiFe	5.0	67.9	[36]
Chitosan/microbial (B. *longum*) composite	4.5	3.93	[37]
Chitosan (10 %)-bentonite (90 %) composite	4.5	46.6	[38]
Polypyrrole-based activated carbon	5.5	50	[39]
Bamboo-biochar	3	183.6	[40]
Ch-A composite beads	4.5	279	This study

To understand the kinetic mechanism of the adsorption process, the fit of the experimental data to pseudo first order (PFO) [41], pseudo second order (PSO) [42], and intra particle diffusion (IPD) [43] models was investigated (**Figure 8**). As presented in **Table 3**, the PFO model shows better agreement with the kinetic data. The PFO model exhibits a high correlation (R^2 =0.967) and closeness of experimental and theoretical adsorption capacities. These results demonstrate the applicability of the PFO model to explain and interpret the adsorption process.

Two linear regions were identified by applying the IPD model presented in **Figure 8** to experimental data. The IPD model rate constants are calculated from the slopes of the corresponding linear regions. k_{i1} and k_{i2} represent the diffusion rates at different stages of

adsorption. In the initial stage, Pb^{2+} ions were adsorbed very rapidly onto the outer surface of the Ch-A composite. After the active centers on the outer surface of the composite were occupied, intraparticle diffusion occurred more slowly. The IPD model fit graph in **Figure 8** shows that the linear regions do not pass through the origin, indicating that the Pb^{2+} adsorption mechanism occurs through multiple mechanisms, such as pore diffusion and film diffusion.

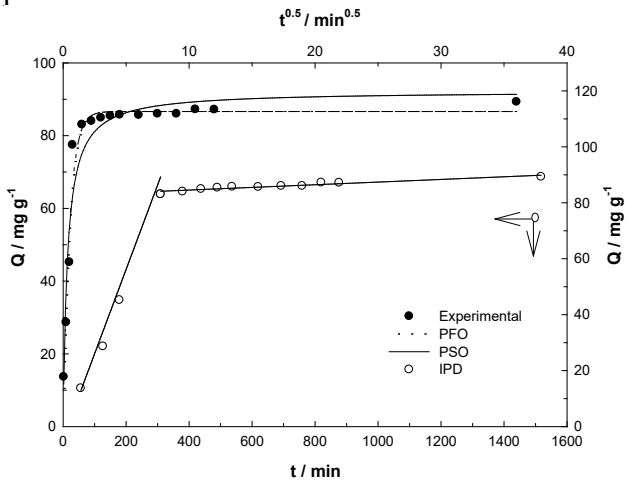


Figure 8. Adsorption kinetic models

Table 3. Parameters of kinetic models

Kinetic model	Parameter	Value
PFO	Q_t/mg g^{-1}	87.3
$Q_t = Q_e[1 - e^{-k_1 t}]$	Q_e/mg g^{-1}	86.6
$H_1 = k_1 Q_e$	k_1/min^{-1}	0.0482
	H_1/mgg^{-1}min^{-1}	4.17
	R^2	0.967
PSO	Q_t/mgg^{-1}	87.3
$Q_t = \frac{t}{\left[\frac{1}{k_2 Q_e^2}\right] + \left[\frac{t}{Q_e}\right]}$	Q_e/mgg^{-1}	92.3
	k_2/mg^{-1}gmin^{-1}	7.9x10^4
$H_2 = k_2 Q_e^2$	H_2/mgg^{1}min^{-1}	6.73
	R^2	0.937
IPD	k_1/mgg^{-1}min$^{-0.5}$	0.0827
$Q_t = k_i t^{0.5}$	k_2/mgg^{-1}min$^{-0.5}$	0.00408
	R^2	0.899

3.6. Effect of Temperature

The effect of ambient temperature on Pb^{2+} adsorption onto Ch-A composite was investigated at 5 ºC, 25 ºC, and 40 ºC, while keeping other parameters ([Pb^{2+}]$_0$: 1000 mg L^{-1}, m: 5 g L^{-1}, pH: 4.5, t: 24 h) constant. The relationship between, which expresses the substance distribution in equilibrium between the adsorbent and the solution obtained at these temperatures, was examined graphically. The ΔH^0 and ΔS^0 parameters were determined from the slope and intercept of this graph using the following equations (**Eq. 3-5**) [44].

$$K = \frac{Q}{C_e} \quad (3)$$

$$lnK = \frac{\Delta S^0}{R} - \frac{\Delta H^0}{RT} \quad (4)$$

$$\Delta G^0 = -RTlnK \quad (5)$$

Table 4 details the calculated thermodynamic parameters for the adsorption process. **Figure 9** shows a significant increase in adsorption capacity as the temperature increases from 5 °C to 40 °C. This trend demonstrates that the adsorption process is endothermic, as increasing temperature increases the energy level of the system, facilitating ion adsorption. On the other hand, the positive ΔH^0 value confirms that the system absorbs heat from the external environment, indicating an endothermic character. The negative ΔG^0 values obtained at 5 °C, 25 °C, and 40 °C indicate that the adsorption of Pb^{2+} ions onto the Ch-A composite occurs spontaneously.

Furthermore, the positive ΔS^0 value indicates increased disorder in the system. This can be explained by the fact that, as Pb^{2+} ions migrate from solution to the adsorbent surface during adsorption, the water molecules in the surrounding hydration shell are released. This increases the total entropy of the system, and the ions become freer. This finding demonstrates that the adsorption process is favorable not only in terms of energy but also in terms of increased disorder.

3.7. Possible Adsorption Mechanism

The adsorption capacity of an adsorbent is governed by the interactions between the adsorbate and the functional groups present on the adsorbent surface. The Ch-A composite surface is rich in functional groups such as –NH_2, –COOH, and –OH, which exhibit a strong affinity for Pb^{2+} ions. Electrostatic interactions are established between these functional groups and Pb^{2+} ions, facilitating their adsorption on the Ch-A composite surface.

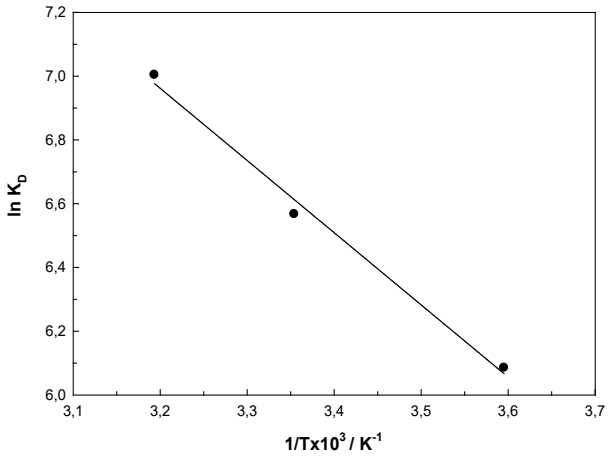


Figure 9. The effect of temperature on the adsorption

Table 4. Thermodynamic parameters

T/°C	ΔH^0 (kJmol^{-1})	ΔG^0 (kJmol^{-1})	ΔS^0 (Jmol^{-1}K^{-1})	R^2
5		-14.0		
25	18.8	-16.4	118	0.993
40		-18.2		

Following Pb^{2+} adsorption, the FT-IR spectrum of the Ch-A composite revealed significant shifts in the locations and intensity changes of the characteristic absorption peaks corresponding to amino, carboxyl, and amide groups. These spectral changes can be attributed to the formation of electrostatic interactions and complexation between Pb^{2+} ions and the surface functional groups of the composite. In particular, the adsorption of Pb^{2+} ions occurs primarily through the complexation of the -NH_2 and -COOH groups on the surface with Pb^{2+} ions, forming stable metal-ligand bonds. After Pb^{2+} ion adsorption, the Ch-A composite surface appears smoother in the SEM morphology, further supporting the formation of surface complexation.

Furthermore, EDX analysis reveals that the Na peaks disappear and prominent Pb peaks appear after Pb^{2+} adsorption, indicating that ion exchange plays a crucial role in the overall adsorption process. In light of all this, the dominant mechanisms for Pb^{2+} ions adsorbed by the cross-linked Ch-A composite beads are suggested to be pore diffusion, film diffusion, electrostatic attraction, ion exchange, and surface complexation (**Figure 10**). These mechanisms act synergistically to facilitate the effective binding of Pb^{2+} ions from the aqueous solution to the surface of the composite material.

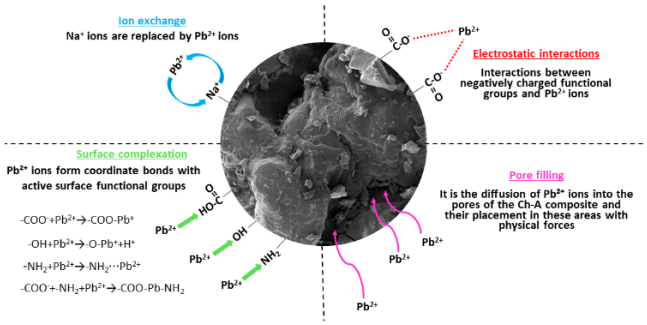


Figure 10. Possible mechanism for Pb^{2+} ion adsorption onto Ch-A composite

5. Conclusion

In this study, a chitosan-alginate composite was successfully produced by using ECH and TPP crosslinkers. The composite exhibited remarkable Pb^{2+} adsorption performance. The composite beads showed excellent adsorption performance with a maximum capacity of 279 mg g^{-1} according to the Langmuir isotherm model. Thermodynamic and kinetic analyses confirmed that the adsorption process was endothermic, spontaneous, and governed by multiple mechanisms, including pore and film diffusion. In addition, FT-IR, SEM-EDX, and pH_{pzc} structural analysis results indicated that electrostatic attraction, ion exchange, and surface complexation act synergistically during the adsorption process to facilitate the effective adsorption of Pb^{2+} ions. These findings indicate that Ch-A composite beads are promising and sustainable adsorbents for the removal of heavy metals from wastewater systems

Article Information From

Acknowledgments
TUBITAK-2209A Research Projects Commission supported the present study.

Authors' Contribution
BA: experimental work, sample preparation, ZMŞ: conceptualization, investigation, data curation, methodology, writing, guidance, editing, review, and supervision.

The Declaration of Conflict of Interest/ Common Interest

Authors have declared no conflict of interest or common interest.

Artificial Intelligence Statement

No artificial intelligence tools were used while writing this article.

Copyright Statement

Authors own the copyright of their work published in the journal and their work is published under the CC BY-NC 4.0 license.

References

[1] K. Raj and A. P. Das, "Lead pollution: Impact on environment and human health and approach for a sustainable solution," *Environ. Chem. Ecotoxicol.*, vol. 5, pp. 79–85, Dec. 2023, doi: 10.1016/j.enceco.2023.02.001.

[2] Poonam, S. K. Bharti, and N. Kumar, "Kinetic study of lead (Pb^{2+}) removal from battery manufacturing wastewater using bagasse biochar as biosorbent," *Appl. Water Sci.*, vol. 8, no. 4, Art. no. 119, Jul. 2018, doi: 10.1007/s13201-018-0765-z.

[3] B. Jagetiya and S. Kumar, "Phytoremediation of lead: A review," in *Lead in Plants and the Environment*, pp. 171–202, Oct. 2020, doi: 10.1007/978-3-030-21638-2_10

[4] RR. N. Khalef, A. I. Hassan, and H. M. Saleh, "Heavy metal's environmental impact," in *Environmental Impact and Remediation of Heavy Metals*. London, U.K.: IntechOpen, Apr. 2022, doi: 10.5772/intechopen.103907.

[5] I. R. Chowdhury, S. Chowdhury, M. A. J. Mazumder, and A. Al-Ahmed, "Removal of lead ions (Pb^{2+}) from water and wastewater: A review on the low-cost adsorbents," *Appl. Water Sci.*, vol. 12, no. 8, Art. no. 185, Aug. 2022, doi: 10.1007/s13201-022-01703-6.

[6] Y. Sayato, "WHO guidelines for drinking-water quality," *Eisei Kagaku*, vol. 35, 1989, doi: 10.1248/jhs1956.35.307.

[7] N. Abdullah, N. Yusof, W. J. Lau, J. Jaafar, and A. F. Ismail, "Recent trends of heavy metal removal from water/wastewater by membrane technologies," *J. Ind. Eng. Chem.*, vol. 76, pp. 17–38, Aug. 2019, doi: 10.1016/j.jiec.2019.03.029

[8] A. Azimi, A. Azari, M. Rezakazemi, and M. Ansarpour, "Removal of heavy metals from industrial wastewaters: A review," *ChemBioEng Rev.*, vol. 4, no. 1, pp. 37–59, Feb. 2017, doi: 10.1002/cben.201600010.

[9] N. A. A. Qasem, R. H. Mohammed, and D. U. Lawal, "Removal of heavy metal ions from wastewater: A comprehensive and critical review," *npj Clean Water*, vol. 4, no. 1, Art. no. 36, Jul. 2021, doi: 10.1038/s41545-021-00127-0.

[10] A. Kumar, R. Indhur, A. G. Sheik, S. B. N. Krishna, S. Kumari, and F. Bux, "A review on conventional and novel adsorbents to boost the sorption capacity of heavy metals: Current status, challenges and future outlook," *Environ. Technol. Rev.*, vol. 13, no. 1, pp. 521–543, Feb. 2024, doi: 10.1080/21622515.2024.2377801.

[11] Q. Zia, M. Tabassum, H. Gong, and J. Li, "A review on chitosan for the removal of heavy metal ions," *J. Fiber Bioeng. Informatics*, vol. 12, no. 3, pp. 103–128, Aug. 2019, doi: 10.3993/JFBIM00301.

[12] X. Q. Liu, X. X. Zhao, Y. Liu, and T. Zhang, "Review on preparation and adsorption properties of chitosan and chitosan composites," *Polym. Bull.*, vol. 79, no. 4, pp. 2633–2665, Mar. 2022, doi: 10.1007/s00289-021-03626-9.

[13] S. Bairagi, S. Banerjee, D. M. Mulvihill, S. Ahmed, and S. W. Ali, "Extraction, structural properties, and applications of sodium alginate," in *Natural Gums: Extraction, Properties, and Applications*, pp. 599–618, Jul. 2023, doi: 10.1016/B978-0-323-99468-2.00022-X.

[14] S. Liu, Y. Li, and L. Li, "Enhanced stability and mechanical strength of sodium alginate composite films," *Carbohydr. Polym.*, vol. 160, pp. 62–70, Dec. 2017, doi: 10.1016/j.carbpol.2016.12.048

[15] I. M. Savić Gajić, I. M. Savić, and Z. Svirčev, "Preparation and characterization of alginate hydrogels with high water-retaining capacity," *Polymers*, vol. 15, no. 12, Art. no. 2592, Apr. 2023, doi: 10.3390/polym15122592.

[16] K. Sakugawa, A. Ikeda, A. Takemura, and H. Ono, "Simplified method for estimation of composition of alginates by FTIR," *J. Appl. Polym. Sci.*, vol. 93, no. 3, pp. 1372–1377, May 2004, doi: 10.1002/app.20589

[17] A. Pawlak and M. Mucha, "Thermogravimetric and FTIR studies of chitosan blends," *Thermochim. Acta*, vol. 396, no. 1–2, pp. 153–166, Dec. 2003, doi: 10.1016/S0040-6031(02)00523-3.

[18] X. Yang, T. Zhou, B. Ren, A. Hursthouse, and Y. Zhang, "Removal of Mn(II) by sodium alginate/graphene oxide composite double-network hydrogel beads from aqueous solutions," *Sci. Rep.*, vol. 8, no. 1, Art. no. 10717, Jul. 2018, 05539-9, doi: 10.1038/s41598-018-29133-y.

[19] Z. M. Şenol and H. Arslanoğlu, "Influential biosorption of lead ions from aqueous solution using sand leek (*Allium scorodoprasum* L.) biomass: Kinetic and isotherm study," *Biomass Convers. Biorefinery*, vol. 15, no. 6, pp. 8809–8819, Mar. 2025, doi: 10.1007/s13399-024-05539-9.

[20] D. Kovačević, A. Pohlmeier, G. Özbaş, H. D. Narres, and M. J. N. Kallay, "The adsorption of lead species on goethite," *Colloids Surf. A Physicochem. Eng. Asp.*, vol. 166, no. 1–3, pp. 225–233, Jun. 2000, doi: 10.1016/S0927-7757(99)00449-5.

[21] M. Mullet, P. Fievet, A. Szymczyk, A. Foissy, J.-C. Reggiani, and J. Pagetti, "A simple and accurate determination of the point of zero charge of ceramic membranes," *Desalination*, vol. 121, no. 1, pp. 41–48, Jan. 1999, doi: 10.1016/S0011-9164(99)00006-5.

[22] I. Langmuir, "Adsorption of gases on glass, mica and platinum," *J. Am. Chem. Soc.*, vol. 40, no. 9, pp. 1361–1403, 1918.

[23] H. Freundlich, "Über die Adsorption in Lösungen," *Z. Phys. Chem.*, vol. 57, no. 1, pp. 385–470, Jan. 1907, doi: 10.1515/zpch-1907-5723.

[24] Q. Hu and Z. Zhang, "Application of Dubinin–Radushkevich isotherm model at the solid/solution interface: A theoretical analysis," *J. Mol. Liq.*, vol. 277, pp. 646–648, Mar. 2019, doi: 10.1016/j.molliq.2019.01.005.

[25] T. K. Naiya, P. Chowdhury, A. K. Bhattacharya, and S. K. Das, "Saw dust and neem bark as low-cost natural biosorbent for adsorptive removal of Zn(II) and Cd(II) ions from aqueous solutions," *Chem. Eng. J.*, vol. 148, no. 1, pp. 68–79, May 2009, doi: 10.1016/j.cej.2008.08.002.

[26] E. Radha, T. Gomathi, P. N. Sudha, S. Latha, A. A. Ghfar, and N. Hossain, "Adsorption studies on removal of Pb(II) and Cd(II) ions using chitosan derived copolymeric blend," *Biomass Convers. Biorefin.*, vol. 15, no. 2, pp. 1847–1862, Oct. 2025, doi: 10.1007/s13399-021-01918-8.

[27] L. Ton-That, T.-P.-T. Nguyen, B.-N. Duong, D.-K. Nguyen, N.-A. Nguyen, T. Ho, and V. P. Dinh, "Insights into Pb(II) adsorption mechanisms using jackfruit peel biochar activated by a hydrothermal method toward heavy metal removal from wastewater," *Biochem. Eng. J.*, vol. 212, Art. no. 109525, Dec. 2024, doi: 10.1016/j.bej.2024.109525.

[28] B. Chen, H. Zhao, S. Chen, F. Long, B. Huang, B. Yang, and X. Pan, "A

magnetically recyclable chitosan composite adsorbent functionalized with EDTA for simultaneous capture of anionic dye and heavy metals in complex wastewater," *Chem. Eng. J.*, vol. 356, pp. 69–80, Jan. 2019, doi: 10.1016/j.cej.2018.08.222.

[29] Y. Huang, Y. Shen, G. Zhang, P. Lu, Z. Wu, R. Tang, J. Liu, X. Wu, C. Wang, and H. Zheng, "Highly effective and selective removal of lead ions by polymer-grafted silica-coated acid-resistant magnetic chitosan composites," *Sep. Purif. Technol.*, vol. 314, Art. no. 123561, Jun. 2023, doi: 10.1016/j.seppur.2023.123561.

[30] R. El Kaim Billah, M. A. Islam, M. Agunaou, and A. Soufiane, "A promising chitosan/fluorapatite composite for efficient removal of lead(II) from an aqueous solution," *Arab. J. Geosci.*, vol. 14, no. 12, Art. no. 1134, Jun. 2021, doi: 10.1007/s12517-021-07473-w.

[31] E. Cheraghipour and M. Pakshir, "Process optimization and modeling of Pb(II) ions adsorption on chitosan-conjugated magnetite nano-biocomposite using response surface methodology," *Chemosphere*, vol. 260, Art. no. 127560, Dec. 2020, doi: 10.1016/j.chemosphere.2020.127560.

[32] W. Shenjin, L. Xiaoxi, Z. Chenyang, H. Wenjihao, L. Yaochi, F. Xinzhuang, Y. Jun, and S. Wei, "Adsorption and selective mechanism of Pb^{2+} and Cd^{2+} on the surface of calcined modified attapulgite," *Sep. Purif. Technol.*, vol. 353, Art. no. 128377, Jan. 2025, doi: 10.1016/j.seppur.2024.128377.

[33] Q. Fu, J. Hu, and S. Zhou, "Adsorption properties of graphene oxide@sodium alginate composite for Pb(II)," *J. Iran. Chem. Soc.*, vol. 21, no. 2, pp. 399–407, Dec. 2024, doi: 10.1007/s13738-023-02932-5.

[34] Y. Fang, L. Yang, F. Rao, Y. Zheng, and Z. Song, "Adsorption behavior and mechanism of MB, Pb(II) and Cu(II) on porous geopolymers," *Ceram. Int.*, vol. 51, no. 9, pp. 11455–11466, Apr. 2025, doi: 10.1016/j.ceramint.2024.12.564.

[35] Y. Du, Y. Xu, J. Hou, X. Li, J. Yang, J. Yang, S. Shan, C. Wang, and H. Su, "Robust fabrication of pyrogallol-conjugated dextran hydrogel as antioxidant hemo-adsorbent for the selective adsorption of Pb(II)," *Sep. Purif. Technol.*, vol. 363, Art. no. 132098, Aug. 2025, doi: 10.1016/j.seppur.2025.132098.

[36] S. A. Jasim, K. Hachem, W. K. Abdelbasset, G. Yasin, W. Suksatan, and C. Chen, "Efficient removal of Pb(II) using modified chitosan Schiff base@Fe/NiFe," *Int. J. Biol. Macromol.*, vol. 204, pp. 644–651, Apr. 2022, doi: 10.1016/j.ijbiomac.2022.01.151.

[37] E. Khanniri, M. Yousefi, A. M. Mortazavian, N. Khorshidian, S. Sohrabvandi, M. Arab, and M. R. Koushki, "Effective removal of lead(II) using chitosan and microbial adsorbents: Response surface methodology (RSM)," *Int. J. Biol. Macromol.*, vol. 178, pp. 53–62, May 2021, doi: 10.1016/j.ijbiomac.2021.02.065.

[38] H. Majiya, F. Clegg, and C. Sammon, "Bentonite-chitosan composites or beads for lead (Pb) adsorption: Design, preparation, and characterisation," *Appl. Clay Sci.*, vol. 246, Art. no. 107180, Dec. 2023, doi: 10.1016/j.clay.2023.107180.

[39] A. A. Alghamdi, A. B. Al-Odayni, W. S. Saeed, A. Al-Kahtani, F. A. Alharthi, and T. Aouak, "Efficient adsorption of lead(II) from aqueous phase solutions using polypyrrole-based activated carbon," *Materials*, vol. 12, no. 12, Art. no. 2020, Jun. 2019, doi: 10.3390/ma12122020.

[40] D. T. Nguyen, T. K. Hoang, T. D. Tran, M. H. Nguyen, K. T. Trinh, D. A. Khuong, T. Tsubota, and T. D. Pham, "Adsorption characteristics of individual and binary mixture of ciprofloxacin antibiotic and lead(II) on synthesized bamboo-biochar,"

Environ. Res., vol. 273, Art. no. 121225, May 2025, doi: 10.1016/j.envres.2025.121225.

[41] Y. S. Ho and G. McKay, "Kinetic models for the sorption of dye from aqueous solution by wood," *Process Saf. Environ. Prot.*, vol. 76, no. 2, pp. 183–191, May 1998, doi: 10.1205/095758298529326.

[42] Y. S. Ho and G. McKay, "Pseudo-second order model for sorption processes," *Process Biochem.*, vol. 34, no. 5, pp. 451–465, Jul. 1999, doi: 10.1016/S0032-9592(98)00112-5.

[43] F. C. Wu, R. L. Tseng, and R. S. Juang, "Initial behavior of intraparticle diffusion model used in the description of adsorption kinetics," *Chem. Eng. J.*, vol. 153, no. 1–3, pp. 1–8, Nov. 2009, doi: 10.1016/j.cej.2009.04.042.

[44] E. C. Lima, A. Hosseini-Bandegharaei, J. C. Moreno-Piraján, and I. Anastopoulos, "Critical review of the estimation of the thermodynamic parameters on adsorption equilibria: Wrong use of equilibrium constant in the Van't Hoff equation for calculation of thermodynamic parameters of adsorption," *J. Mol. Liq.*, vol. 273, pp. 425–434, Jan. 2019, doi: 10.1016/j.molliq.2018.10.048.